

2. STRESS INTENSITY FACTOR K_I AND ENERGY RELEASE RATE G IN THE CASE OF A TRANSVERSE CRACK IN A CYLINDRICAL TENSIONED WIRE

by MM. A. ATHANASSIADIS⁽¹⁾, J.M. BOISSENOT⁽²⁾,
P. BREVET⁽¹⁾, D. FRANÇOIS⁽³⁾, A. RAHARINAIVO⁽¹⁾

1 - INTRODUCTION

High strength steel wires or bars may break after cracking due to either fatigue or stress corrosion. Their fracture parameters may then be defined either empirically (1) (2) or by calculations using finite elements (3), because the geometry has not a cylindrical symmetry which may permit an analytical calculation of stresses and displacements.

In this study, we present calculations of stress intensity factor K_I and strain energy release rate G using a numerical method named boundary integral equation method. The calculation results are compared with the experimental data obtained on 12 mm diameter plain carbon steel wires, used for prestressed concrete.

2 - CALCULATIONS OF FRACTURE PARAMETERS

2.1 - Principles

The boundary integral equation method consists of transforming partial differential equations describing the volume of a solid body into integral equations on its boundary (4) (5) (6).

The advantage of this technique is apparent, since it permits us to replace a three-dimensional problem by a two-dimensional one, which simplifies the exploitations of data and of results.

-
- (1) L.C.P.C.
(2) C.E.T.I.M.
(3) U.T.C.

The seeming inconvenience of numerical calculations might come from the difficulty of using the results under conditions different from those which permitted the calculations. In fact, we have to introduce data, such as Young's modulus, which are those of real cases and to choose a sufficient number of configurations (e.g: the shape of the cracks) in such a way that the calculation results may be applied by interpolation.

The program, so called E.I.T.D., used in this study was formerly well settled (5),(6)(11)(12)(13) for linear elasticity problems in a three dimensional space.

2.2 - Data for calculations

Calculations were applied to cylindrical wires, in high strength steel, 80 mm long, having a diameter $D = 2R = 12$ mm, a Young's modulus $E = 210.000$ N/mm² and a Poisson's ratio $\nu = 0,3$.

The crack was located in the middle of the wire length, perpendicularly to its axis and symmetrically with respect to a diametral plane (figure 1).

The crack front was chosen as similar as possible to the actual cracks observed in prestressing cables steels. For describing the various shapes actually observed, the crack front points have, in the crack plane, the polar coordinates r and α verifying :

$$\frac{R^2 \alpha^2}{a^2} + \frac{(R-r)^2}{b^2} = 1$$

where a is called the crack length on the periphery; b the crack depth, R being the wire radius.

2.3 - Modelling the sample

Because of the symmetries, calculations dealt only, with the quarter of the wire, bounded by the crack and its symmetry plane. The surface of this solid is cut ("discretized") into triangles and quadrangles ("isoparametrical elements") (figure 2)

In every "element" contiguous to the crack front (figure 3), thenodes corresponding to the middles of the sides perpendicular to the front are located at the quarter of the side length, near the crack front. This artifice, used by other workers (14), permits us to correctly describe the displacement field.

The complete meshing includes in average 45 "elements" and 128 "nodes".

Three types of loadings were studied : tension, compression and pure bending. Only the results corresponding to the tension loading (calculations and experimentations) are indicated.

2.4 - Definitions of the calculated parameters

We assume that the elements of the diametral plane (axes 1-3) move in their own plane. The motions of the points on the crack remain free, as any bulk motion of the piece is avoided.

Under those conditions, the E.I.T.D. program permits us to calculate the potential energy P of the cracked wire starting from the displacement and stresses at every node.

We define the stress intensity factor K_I in directions perpendicular to the crack front, at each crack front point, as :

$$K_I = \lim_{r \rightarrow 0} \sqrt{\frac{2\pi}{r}} E' u_3(r, \theta = \pi) \quad (2)$$

with $E' = E$ in plane stress field, i.e. at the wire periphery

$E' = \frac{E}{1-\nu^2}$ in plane strain field, at the core of the wire.

Besides, the energy is $\Psi = \frac{1}{2} \sigma_{ij} \epsilon_{ij}$ and the potential energy

$$P = \int_V w \, dV - \int_V f_i u_i \, dV - \int_S T_i u_i \, dS \quad (3)$$

where S is the surface, V the volume, u_i the displacement T_i ; the surface tension, f_i the bulk body forces.

The potential energy P is a polynomial versus parameters a and b .

The strain energy rate is $G = \sup \left(-\frac{dP}{dS} \right)$ (4)

where dS is the virtual increase of the cracked area.

2.5 - Calculation results

The figure 4 shows an example of the K_I variation along a crack front, calculations having used the displacements u .

It therefore appears that K_I varies along the crack front.

We defined at each point $G_i = \frac{K_{Ii}^2}{E'}$ (5)

and a parameter $G^* = \frac{1}{2S} \int_{-S}^{+S} G_i dS$ (6)

which gives the strain energy release rate versus the geometry (figure 6).

3 - TENSILE TESTS EXPERIMENTATIONS

Experimentations were carried out using a plain carbon steel wire, 1.2 mm diameter, with an ultimate tensile stress of about 1500 N/mm².

It was not possible to check the K_I local values. Therefore experimentations dealt with the determination of G using the compliance method.

Compliance C is defined using $u_i = C T_i$, the strain energy release rate

$$G = \frac{1}{2} T_i \frac{du_i}{dS} = \frac{1}{2} T_i^2 \frac{dC}{dS} \quad (7)$$

The wire with a crack having an area S , has a compliance $C(S)$ (figure 5). Experimentally, it deals with sharp notches with a circular front, obtained by spark erosion (18). The experimental values of the strain energy release rate are noted G^{++} (Table 1).

4 - COMPARISON OF G MEASUREMENT METHODS

The table 1 gives the comparison of the methods of determining the strain energy release rate, according to formula (4), the formula (6) and experimentally.

It appears there is a good agreement between those three methods.

5 - CRACK PROPAGATION BY FATIGUE

5.1 - Calculations

This part of the study deals with the propagation of the here above describe defects (figure 1) when a cyclic loading is applied to the wire. The calculation of this propagation uses a method formerly settled (13). The evolution criterion is the one which was proposed by Lemaitre (16): "among every possible increment of a same area dS of a crack, the actual increment is the one which yields the maximum of the potential energy variation rate".

The criterion is written according to the following relations :

$$\left. \begin{aligned} dS &= \frac{\pi}{4} (ab - a_0 b_0) - \frac{1}{3} R (ab^2 - a_0 b_0^2) \\ G &= \sup \left(-\frac{dP}{dS} \right) \end{aligned} \right\} (8)$$

$$\left. \begin{aligned} \text{with the inequalities } da &= a - a_0 \geq 0 \\ db &= b - b_0 \geq 0 \\ G &\leq G_c \end{aligned} \right\} (9)$$

It is proper to note that the quantity $\sup \left(-\frac{dP}{dS} \right)$ rigorously is not related to the assumptions made on dS . In searching for the maximum, we assumed that dS is constant and thus da and db are related. This assumption might introduce errors which must be evaluated with experimental checks. Generally $\sup \left(-\frac{dP}{dS} \right)$ is calculated using an objective norm depending on the parameters which describe the crack front.

The stress intensity factor has a mean value

$$\bar{K} = \sqrt{\frac{EG}{1-\nu}} \quad (10)$$

and during the cyclic loading the range of \bar{K} is

$$\Delta \bar{K} = \bar{K}_{\max} - \bar{K}_{\min} \quad (11)$$

The calculations of the crack propagation assume a law $\frac{dS}{dN} = C (\Delta \bar{K})^m$ where C and m are constants depending on the material. For the studied steel, using comparison with analogous steels, we assumed $C = 8.10^{-2}$, $m = 4$ in SI units.

Resolving the equations (8) needs the potential energy $P(a,b)$ to be known. The strain energy release rate G is calculated using an iterative method and an integration of the fatigue differential equation according to Range Kubba method.

At the starting point, the initial defects have various shapes. Their propagation was calculated under repeated tensioning ($\bar{K}_{\min} = 0$).

The figure 7 shows an example of a calculated growth of a defect.

As a general rule, the ratio $\frac{b}{a}$ tends to become stable about 0,75, value which corresponds to the uniform K_I distribution along the crack front.

Thus, following calculations, fracture occurs when the crack has a ratio $\frac{b}{a} = 0,75$ and such an area as

$$G(a, b) = G_c.$$

5.2 - Oscillating tensioning experimentations

Oscillating tensioning fatigue tests were carried out on wires for prestressing concrete described above. The applied stress varied between $0,3 R_m$ and $0,5 R_m$, R_m being the ultimate tensile stress.

Wires had notches obtained after spark erosion, and the study included 10 wires with various notches.

The figures 8 et 9 show the defect growth until specimens break. The observed crack corresponds to $\frac{b}{a} = 0,75$ and to a toughness $G_c = 27 \pm 3 \text{ M Pa m}^{\frac{1}{2}}$ ($K_{IC} = 79 \pm 4 \text{ M Pa m}^{\frac{1}{2}}$).

This value is practically equal to the one which was obtained on the same steel, using circular cracks obtained after rotative bending fatigue and for which

$$K_{IC} = 80 \pm 4 \text{ M Pa m}^{\frac{1}{2}}$$

These experimental results are to be compared with the calculation results in repeated tensioning (with the same stress range $\Delta\sigma$).

The cycles numbers at failure (N_f) are in good agreement. In table 2 the calculated N_f corresponds to $G = G_c$.

6 - CONCLUSIONS

The calculations of stress intensity factors K_I and of strain energy release rate G were carried out for 20 configurations of lateral cracks in cylindrical wires. This study permits us to draw abacuses giving the values of those parameters for various crack shapes, similar to those which are actually observed. The calculation results agree with those which were obtained by other authors (3) (17) using finite elements and slightly different cracks.

Those abacuses may have practical applications for they relate the critical size (b_c) of a defect having a given shape (b/a ratio) and the toughness (G_c) of a wire (diameter D).

Those calculations have been experimentally confirmed using the compliance method and tensile tests on cracked wires (mode I opening). The experimental results agree with those we formerly published (9).

Besides, the calculations of a crack growth by fatigue show that its shape tends to become stable and to be a configuration for which the stress intensity factor K_I varies very little along the crack front.

Fatigue tests under oscillating tension confirm the existence of that stable shape of the cracks. They also show that fracture occurs when the strain energy release rate G is equal to a constant G_c independent of the initial crack.

REFERENCES

- 1/ - BRACHET M. - Annales de l'Institut Technique du Bâtiment et des Travaux Publics 1977. N° 348 sup. P. 30-50.
- 2/ - RAHARINAIVO A. Utilisation des concepts de la mécanique de la rupture par l'exploitation des essais classiques de corrosion sous tension. -Corrosion, Traitement, Protection, Finition. Vol.20 (1972). P. (276-284)
- 3/ - ASTIZ M.A. (1976). Estudio de la estabilidad de una fisura superficial en un alambre de acero de alta resistencia Tesis defendida en la Escuela T.S. de Ingenieros de Caminos, Canales y Puertos, Universidad Politécnica de Madrid.
- 4/ - CRUSE T.A. Application of the boundary integral equation method to three dimensional stress analysis. Computers and structures. Vol.3. 1973.
- 5/ - LACHAT J.C. , WATSON J. "Application de la méthode des équations intégrales au calcul des structures". Mémoire Technique du CETIM n° 25, Mars 1976.
- 6/ - LACHAT J.C. , WATSON J., "Effective numerical treatment of boundary integral equations : a formulation for 3 - D elastostatics". I.J. for Numerical in Engineering 1976, Vol.10, p 991 - 1005.

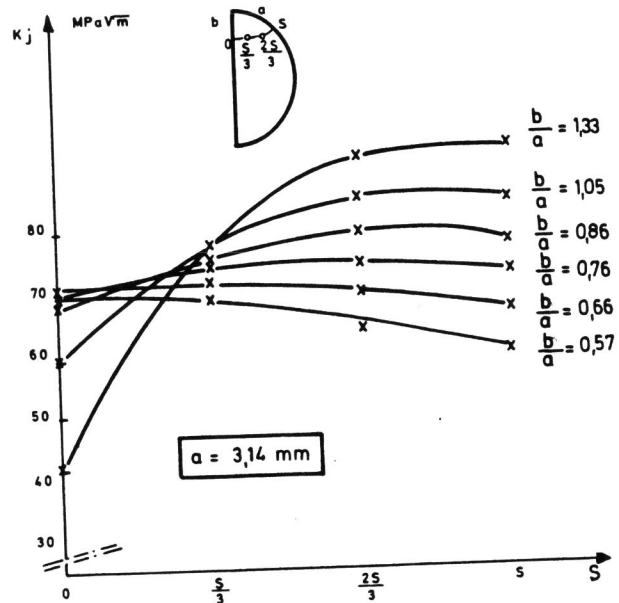
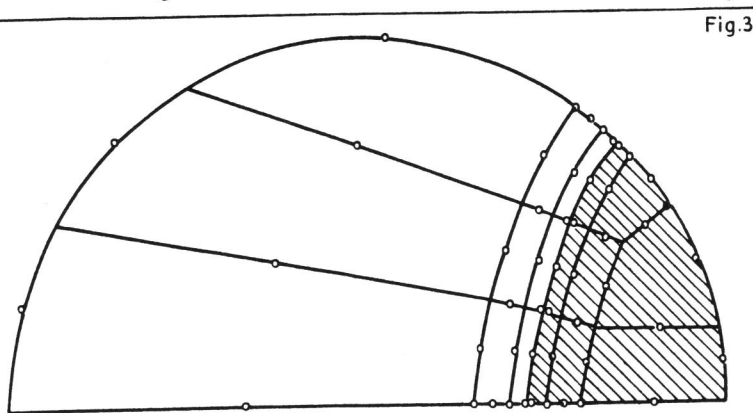
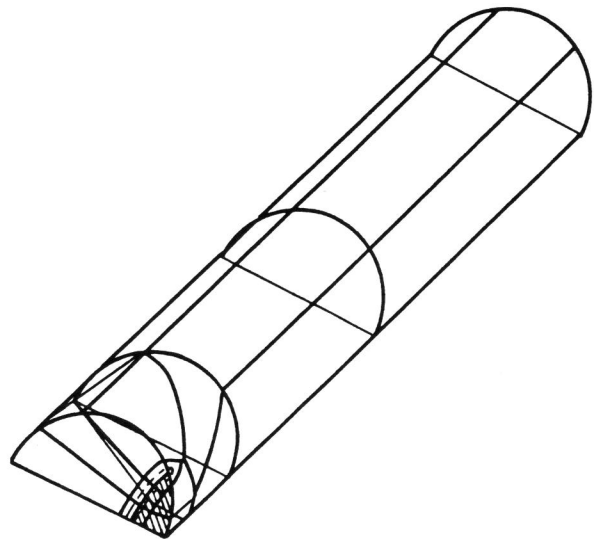
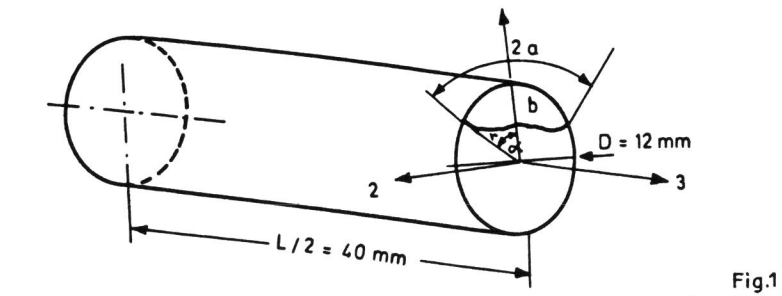
- 7/ - ROOKE D.P., CARTWRIGHT D.J., "Compendium of stress intensity factors London 1976 H.M.S.O.
- 8/ - BUI H.D. "Mécanique de la rupture fragile". Masson et Cie PARIS 1978.
- 9/ - BREVET P., CONDET. P., FRANCOIS. D., RAHARINAIVO.A. Métaux Corrosion. Industrie 1978. - n° 632 - P. 138 - 143 -
- 10/ - SIH G. Methods of analysis and solutions of. Crack problems Noodhoff Mechanics of Fracture 1 1973.
- 11/ - BOISSENOT J.M., GAZAGNE L., LANGE D. Some industrial applications of the boudary integral technique in the of 3-D elastostatics - Proceeding of Int. Symposium on Innovative Numerical Analysis in Applied Engineering Science - Versaille France 23-27 Mai 1977.
- 12/ - BOISSENOT J.M. LANGE D. - Méthodes des équations intégrales et leurs applications. Revue Technique SULZER n° Spécial Recherche (to be published).
- 13/ - BOISSENOT J.M. - Three dimensional analysis of fatigue propagation of a semi-elliptic de fect. Proceedings of IACA Sumposium - Vienne 10-13/10/1977.
- 14/ - HENSHELL R.D. and SHAW K.G., "Crack tip finite elements are unnecessary". Int.J. Num Meth Engng (1975) 9, 495-507.
- 15/ - WEAVER J., "Three dimensional crack analysis". Int. J. Solids Structures 1977, 13, 321-330.
- 16/ - LEMAITRE J. Extension de la notion de taux d'énergie de fissuration aux problèmes trédimensionnels et non-linéaires. Comptes rendus de l'Académie des Sciences T. 282 B (1976) 157-160.
- 17/ - BLACKBURN W.S. "Calculation of Stress intensity factors for straight cracks in grooved and ungrooved shafts" Engin. Fracture Mechanics - 1976. Vol.8. - P. 731-736.

α mm	b mm	$G = \sup \left[\frac{dP}{ds} \right]$ k Pa.m	$G^* = \frac{1}{2s} \int_0^{2s} \frac{k_i^2}{E'} ds$ k Pa.m	$G_{\text{experm.}}$ k Pa.m
0,52	0,40	2,95	3,03	2,80
1,57	1,20	9,33	9,71	9,21
	1,80	11,60	11,88	11,30
3,14	1,80	20,30	18,93	18,15
	2,10	22,14	21,31	20,80
	2,40	24,00	23,30	22,90
	2,70	26,03	25,00	25,80
	3,30	28,05	27,19	28,40
4,71	4,20	29,35	28,81	30,95
	1,80	20,87	19,90	19,10
	2,10	30,52	28,58	27,95
	2,40	33,93	33,07	32,53
	2,70	37,92	37,21	37,50
6,28	3,00	40,92	41,31	41,93
	3,30	44,15	45,48	46,95
	1,20	20,35	18,16	17,80
	2,10	39,82	38,73	37,15
9,42	2,70	54,83	55,07	56,98
	3,30	72,13	73,24	74,90
9,42	1,80	36,95	34,66	-

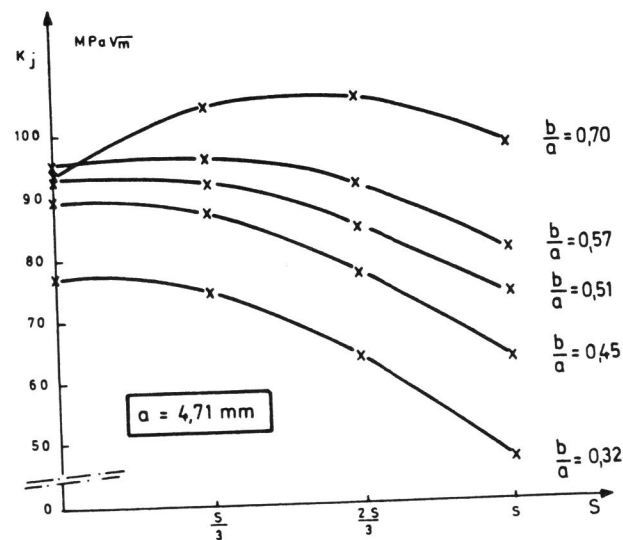
TABLE 1 : Comparison of G values

Initial crack		Final crack			
		Calculations		Experimentations	
a_0 mm	b_0 mm	$\frac{b \text{ (mm)}}{a \text{ (mm)}} = \frac{b}{a}$	N_f (cycles)	$\frac{b \text{ (mm)}}{a \text{ (mm)}} = \frac{b}{a}$	N_f (cycles)
2.05	.6	3.95/5.05=.78	29 500	4.10/5.20=.79	30 300
1.85	.9	3.70/4.93=.75	27 800	3.60/4.70=.76	27 400
2.83	2.4	3.73/5.04=.74	10 900	3.60/4.75=.75	10 400
3.03	3.0	3.78/4.97=.76	9 100	3.90/5.00=.78	9 400
4.33	3.0	3.62/4.96=.73	8 600	3.80/5.07=.75	9 000

Table 2 : Fatigue crack propagation



Figures 4



(B)

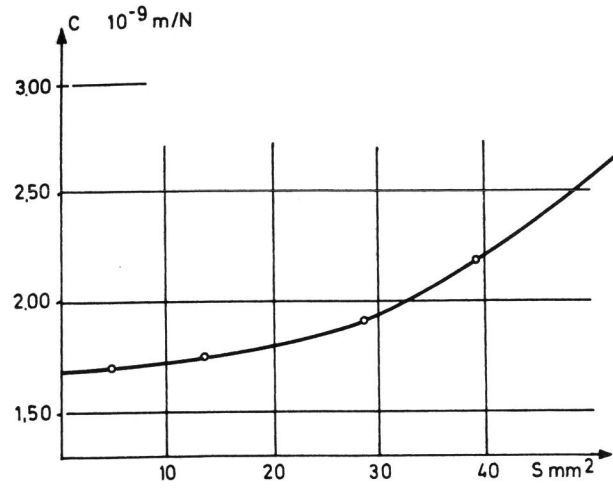


Fig.5

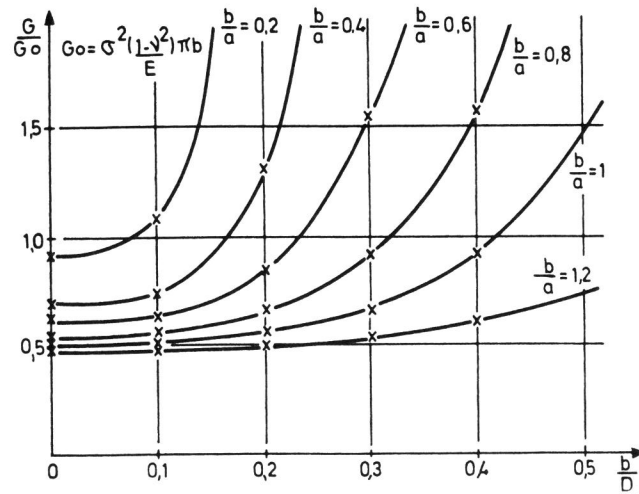
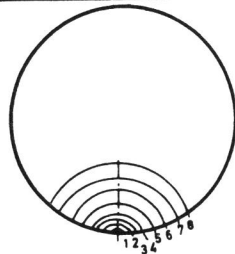


Fig.6



N°	$\frac{b}{a}$	N cycles
1	1,00	100
3	0,82	8900
5	0,81	12700
7	0,77	13200

Fig.7



Figure 8

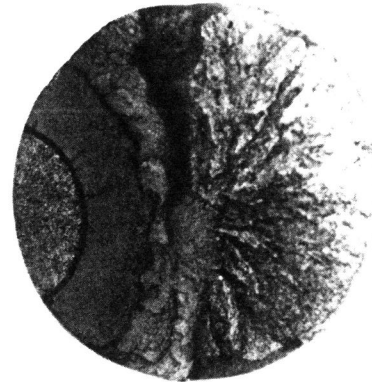


Figure 9